electronics

MDPI

Article

Electrocardiogram-Based Driver Authentication Using Autocorrelation and Convolutional Neural Network Techniques

Giwon Ku [1], Choeljun Choi [1], Chulseung Yang [1], Jiseong Jeong [1], Pilkyo Kim [1], Sangyong Park [1], Taekeon Jung [1] and Jinsul Kim [2,*]

[1] AI Convergence Home Appliance Research Center, Korea Electronics Technology Institute, Gwangju 61011, Republic of Korea; giwon9@keti.re.kr (G.K.); cjchoi@keti.re.kr (C.C.); yangcs@keti.re.kr (C.Y.); json@keti.re.kr (J.J.); pk28@keti.re.kr (P.K.); keti-psy@keti.re.kr (S.P.); taekeon@keti.re.kr (T.J.)

[2] Department of ICT Convergence System Engineering, Chonnam National University, Gwangju 61186, Republic of Korea

* Correspondence: jsworld@jnu.ac.kr

Abstract: This study presents a novel driver authentication system utilizing electrocardiogram (ECG) signals collected through dry electrodes embedded in the steering wheel. Traditional biometric authentication methods are sensitive to environmental changes and vulnerable to replication, but this study addresses these issues by leveraging the unique characteristics and forgery resistance of ECG signals. The proposed system is designed using autocorrelation profiles (ACPs) and a convolutional neural network and is optimized for real-time processing even in constrained hardware environments. Additionally, advanced signal processing algorithms were applied to refine the ECG data and minimize noise in driving environments. The system's performance was evaluated using a public dataset of 154 participants and a real-world dataset of 10 participants, achieving F1-Scores of 96.8% and 96.02%, respectively. Furthermore, an ablation study was conducted to analyze the importance of components such as ACPs, normalization, and filtering. When all components were removed, the F1-Score decreased to 60.1%, demonstrating the critical role of each component. These findings highlight the potential of the proposed system to deliver high accuracy and efficiency not only in vehicle environments but also in various security applications.

Keywords: individual authentication; biometric; electrocardiogram; autocorrelation template

check for updates

Citation: Ku, G.; Choi, C.; Yang, C.; Jeong, J.; Kim, P.; Park, S.; Jung, T.; Kim, J. Electrocardiogram-Based Driver Authentication Using Autocorrelation and Convolutional Neural Network Techniques. *Electronics* **2024**, *13*, 4974. https://doi.org/10.3390/electronics13244974

Academic Editor: Abdur Rasool

Received: 31 October 2024
Revised: 3 December 2024
Accepted: 10 December 2024
Published: 17 December 2024

Copyright: © 2024 by the authors. Licensee MDPI, Basel, Switzerland. This article is an open access article distributed under the terms and conditions of the Creative Commons Attribution (CC BY) license (https://creativecommons.org/licenses/by/4.0/).

1. Introduction

In the era of intelligent electronics, various smart infotainment systems are being implemented in automobiles to enhance driver-centric convenience and safety [1,2]. These technologies range from vehicle control using autonomous driving technologies to providing personalized services for drivers based on biometric information. Biometric information enables the optimization of seat, mirror, and steering wheel positions; the adjustment of interior temperature and comfort settings; and the delivery of personalized entertainment depending on the driver's emotional state and health condition [3].

Driver authentication is the first requirement for providing such personalized services. It serves as a critical tool for preventing identity theft and protecting against data breaches by allowing users to verify their identities. Traditional authentication methods are broadly classified into "knowledge-based" (e.g., passwords), "possession-based" (e.g., cards and keys), and "biometric-based" (e.g., physiological characteristics) categories [4]. However, authentication factors such as passwords and cards are susceptible to loss, theft, and duplication, and the reuse of the same password across multiple systems increases security risks [5]. For these reasons, biometric authentication methods based on unique physiological traits have garnered increasing attention [6]. Biometric information, such as fingerprints, facial features, iris patterns [7], and vein patterns [8], offers high security as it is unique to

each user. However, image-based methods, such as fingerprint and facial recognition, are vulnerable to replication and environmental factors (e.g., lighting and hand conditions) [9].

In response to these limitations, researchers have explored the use of electrocardiogram (ECG) signals for biometric authentication [10,11]. ECG signals, derived from the electrical activity of the heart, possess unique individual characteristics and are difficult to forge [12,13]. Unlike static physiological traits, ECG signals also reflect dynamic cardiac activities, providing high reliability against environmental changes [14]. However, ECG signals are highly variable depending on measurement conditions and individual behaviors, and in vehicular environments, noise generated by driver actions often contaminates the signal [15]. Therefore, research is needed to improve the accuracy and reduce the error rates in such settings.

As a solution to these problems, this study proposes a driver authentication system that combines autocorrelation profiles (ACPs) with a convolutional neural network (CNN) model. ACPs highlight the dynamic features of ECG signals, while the CNN model learns from these data to deliver highly accurate authentication results. The proposed system collects ECG signals through electrodes embedded in the steering wheel of a vehicle and uses signal processing algorithms to minimize environmental noise and artifacts. Subsequently, ACPs and CNN are employed to extract the driver's unique features and perform authentication. The system was validated using a public dataset of 154 participants and a real-world dataset of 10 participants. The results, evaluated through F1-Score metrics, demonstrate that the proposed system is a reliable solution even in challenging environments, such as vehicles.

2. Related Works

Various feature extraction methods are available for ECG-based individual authentication, which can generally be classified into fiducial and non-fiducial methods. Fiducial methods analyze ECG signals by utilizing specific reference points to divide the signals and extract features. The main reference points are the P wave, QRS complex, and T wave, and features such as the onset of waves, peak amplitudes, and intervals between points are extracted [16–21]. This method relies on the accurate detection of reference points, which can achieve high accuracy in some approaches. However, if the reference point detection is inaccurate or the ECG waveform is distorted by noise, the accuracy of the measurements can decrease. Additionally, due to the lack of a clear definition for distinguishing ECG wave boundaries, there can be differences in the methods of specifying the locations of various reference points. Therefore, fiducial methods require robust heart rate segmentation and reference point detection techniques, as well as significant manual feature engineering efforts, which may limit generalization. To improve generalization and reduce manual feature engineering efforts, some studies have introduced non-fiducial strategies. These methods use Fast Fourier Transform (FFT) or wavelet transforms to find features of ECG signals in the frequency domain rather than the time domain [22–26]. Non-fiducial ECG biometric authentication techniques are useful in stable environments as they do not rely on reference points, are simple, and have strong resistance to external interference. Recently, user recognition methods utilizing deep learning have shown excellent performance across various technical fields. In particular, CNN is gaining attention because they can automatically learn inherent patterns from data, preventing the need for manual feature engineering and capturing more hidden patterns. Features of ECG signals are extracted or frequency transformations are performed, and these are then applied to various deep learning models, such as CNN and RNN, for individual identification [9,27–32]. Although existing CNN-based ECG biometric authentication studies have achieved high accuracy, they include complex model structures and a large number of parameters, requiring significant computational resources and large datasets. These models often involve complex data preprocessing and feature extraction processes to prevent overfitting, which may not be suitable for real-time applications or embedded environments.

In this study, we propose a lightweight learning model structure that efficiently processes ECG data for individual authentication within a vehicle, suitable for embedded environments. The proposed model maintains a high performance with fewer parameters and layers, requiring less training data. Performance validation confirmed the high efficiency and performance of the proposed model compared to existing models in terms of size and F1-Score. Additionally, the model demonstrated reliable individual authentication in real-time embedded systems.

3. Methods

This section outlines the key methodologies employed in developing the individual authentication system based on ECG signals collected using dry electrodes embedded in the steering wheel. The study is structured into three main stages, as shown in Figure 1: (1) ECG signal acquisition, (2) signal preprocessing and feature extraction, and (3) model training and authentication. Each stage is designed to achieve the research objectives of high accuracy and real-time authentication while ensuring stable operation in constrained hardware environments. This section provides a detailed explanation of the data processing, analytical procedures, and technologies applied at each stage.

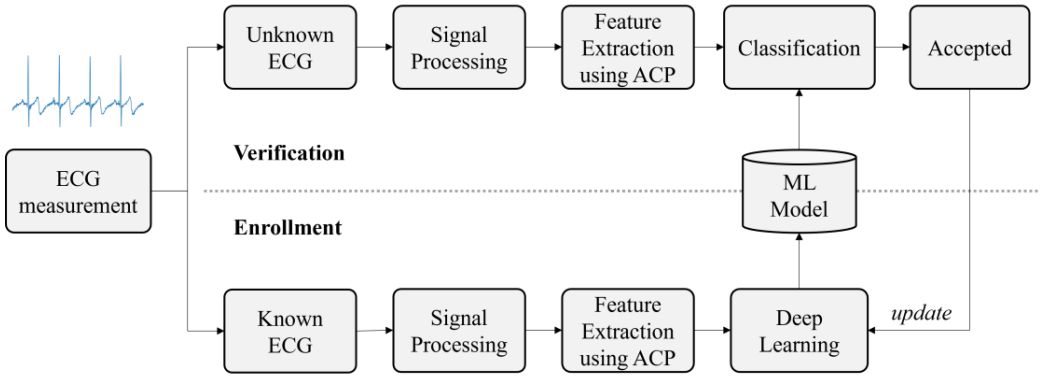


Figure 1. Flowchart of the proposed individual authentication system.

3.1. ECG Measurement

In this study, an individual authentication system was constructed to continuously monitor the driver's health status by collecting ECG data while driving. The proposed system consists of a signal acquisition and analog filtering module, an analog-to-digital converter (ADC), and a Graphics Processing Unit (GPU), as shown in Figure 2.

First, in the ECG Signal Acquisition module, conductive electrodes are attached to acquire the user's biosignals (Figure 2). In the case of conductive electrodes, silver chloride (AgCl) electrodes were selected due to their low skin electrode impedance and high conductivity and stable electrochemical properties. To acquire biological signals, the electrodes are manufactured in a flexible and thin form factor, arranged two on the left and one on the right of the steering wheel, positioned to fit the driver's hands, and continuously acquire ECG data without interfering with driving. The ECG Signal Acquisition module is used to detect the electrical activity of the heart and change it into an electrical signal, and this sensor is designed to precisely measure ECG signals. This module consists of a 0.05~40 Hz bandpass filter (BPF) to effectively separate ECG signals [33,34]. Indeed, 0.05 Hz helps remove DC offset and low-frequency noise, and 40 Hz is applied to minimize frequency noise interference. In addition, a 60 Hz notch filter was added at the rear to remove electrical noise commonly caused by power lines and other electronic devices [35]. Without using a noise removal filter, it can mimic or distort important components of the ECG such as the P or T waves; so, using a notch filter only removes a specific range around 60 Hz and leaves the rest of the ECG signal largely unaffected.

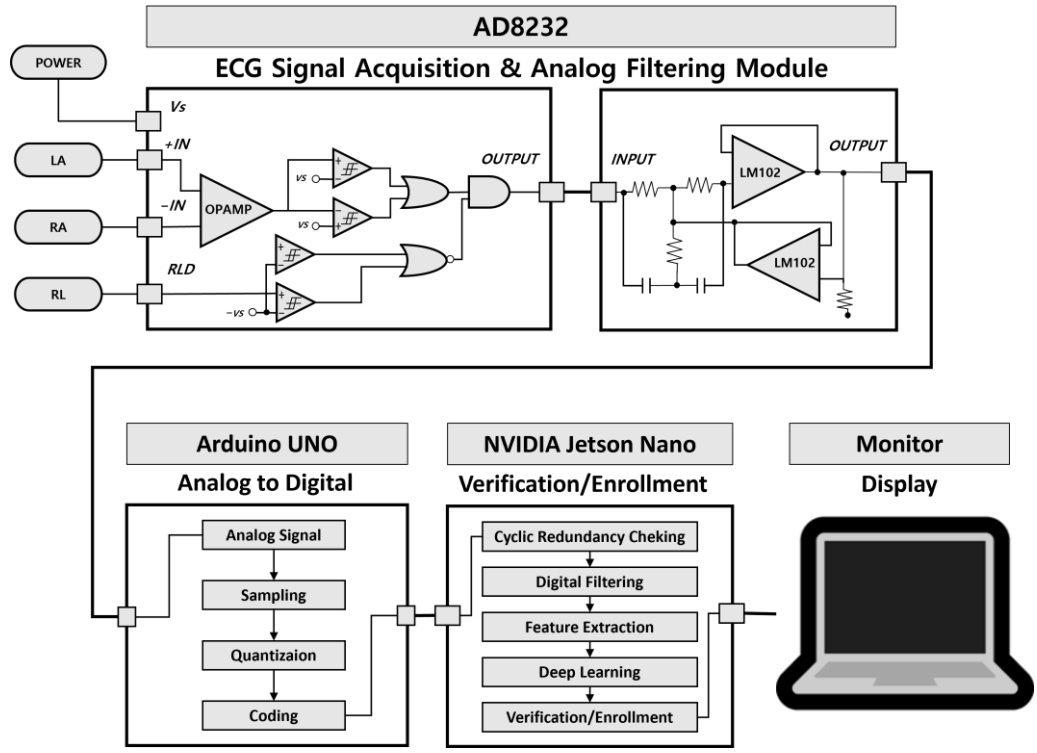


Figure 2. Individual authentication system configuration for steering wheel-based driver identification.

Analog ECG data obtained from the module undergoes analog signal processing and are then converted to digital format through an ADC converter. The ADC used in this system quantifies the analog ECG signal into 1024 individual digital levels with 10-bit resolution. The sampling rate is 100 Hz, and 100 digital data pointers are transmitted per second to the GPU device. GPU devices utilize the PanTompkins algorithm, which is used to detect the QRS complex, which represents the ventricular depolarization phase of the cardiac cycle [36,37]. This algorithm is critical to accurately extracting ECG data by accurately analyzing heart rate patterns and enabling reliable individual authentication.

In the next step, characteristic points such as waveform, periodicity, amplitude, and interval between QRS complexes are extracted from the ECG data to construct a unique ECG profile [38,39]. This profile is stored in the system's database and serves as a biometric template for authentication based on the individual's unique physiological characteristics [16,40]. If a matching profile is identified based on the profiles stored in the database, the system allows access; otherwise, it denies access, enhancing security measures.

3.2. ECG Signal Processing

To measure ECG signals, both analog and digital filters have been implemented to remove noise or unwanted signals that exceed the input signal range. Initially, an analog filter was designed with a cutoff frequency of 0.5 Hz as a second-order high-pass filter to eliminate low-frequency noise. Simultaneously, a second-order low-pass filter with a 40 Hz cutoff frequency was applied to remove noise from the ECG signal.

After processing through the analog filter, the ECG signals converted by the ADC were further refined using a digital filter designed to eliminate noise and filter only the ECG signals. This digital filter comprises a third-order high-pass filter with a 0.5 Hz cutoff frequency and a third-order low-pass filter with a 30 Hz cutoff frequency, which are determined based on the frequency range of the ECG signals.

Additionally, a notch filter was applied to remove the sinusoidal noise occurring at the power line frequencies of 50 Hz or 60 Hz. Both bandpass and notch filters were utilized to enhance the accuracy of the ECG signals and to facilitate easier analysis (Figure 3) [41,42].

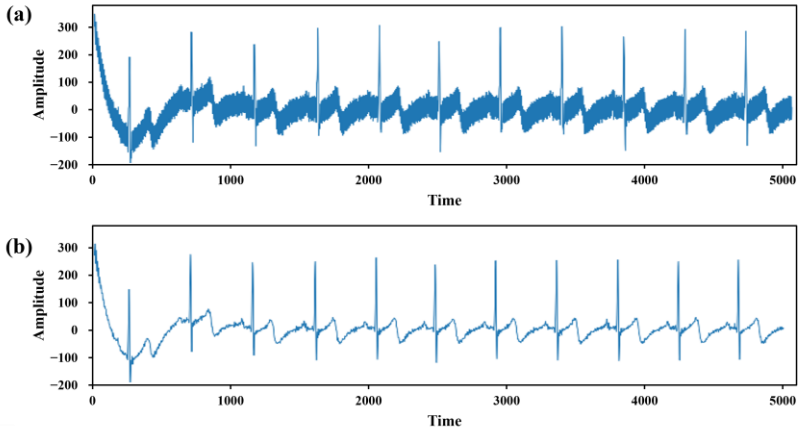


Figure 3. Comparison of ECG signals before and after filtering: (**a**) raw ECG (**b**) filtered ECG.

3.3. Feature Extraction

Feature extraction in ECG signal analysis proceeds in the order of Segmentation, Normalization, and Autocorrelation.

First, Segmentation involves dividing large datasets into smaller, more manageable segments to enable efficient data processing and analysis. For ECG signal feature extraction, it is advisable to segment the data into short durations, but each segment must contain at least one RRI to ensure high authentication accuracy. Typically, the duration to input numbers on a numeric keypad, averaging 5 s, is used as a basis for setting segmentation to 5 s.

Normalization is the process of adjusting data within a specific range or converting it to a standard form. The power values of signals can vary depending on which part of the hand is touched or the humidity of the day. Additionally, the baseline can be affected by motion artifacts. Thus, normalization is performed to reduce the impact of outliers and enable consistent interpretation.

The ACP is a technique used to calculate the self-correlation of time series data, measuring the similarity according to time delays. It is utilized to identify repetitive patterns or the fundamental rhythm in ECG signals by analyzing their auto-correlation properties (Figure 4) [43–45].

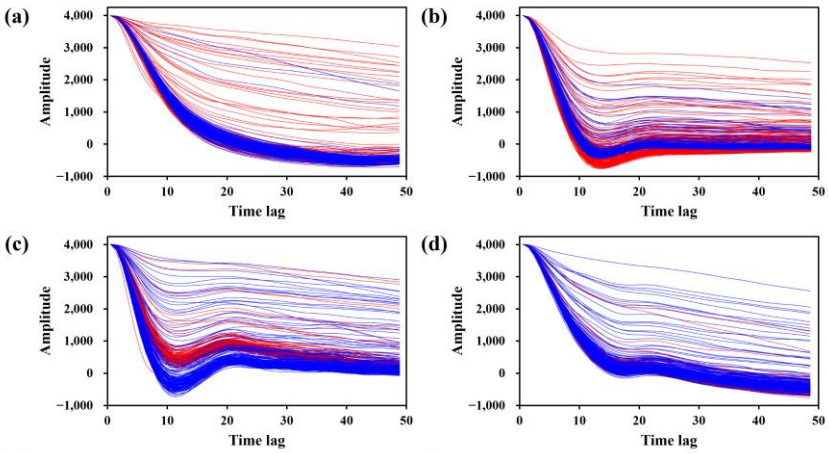


Figure 4. Results of ACPs for ECG signals from four different individuals: (**a**) person 1, (**b**) person 2, (**c**) person 3, and (**d**) person 4. Red line: ACP; Blue line: Average ACP.

3.4. Deep Learning

For individual authentication purposes, we developed a deep learning architecture utilizing CNN specifically tailored to process the ACPs of ECG signals. Inspired by the efficient model architecture of TinySleepNet, which leverages minimalistic yet effective

CNN designs for processing single-channel EEG data [46], our CNN architecture was meticulously crafted to extract distinctive features from the ECG data, crucial for accurately identifying individual identities. We assessed the effectiveness of our model using both publicly available and proprietary datasets specifically collected in our laboratory settings. These datasets enabled us to fine-tune the model across different stages of training, focusing on improving its accuracy during both enrollment and verification phases. The final model was rigorously tested with ECG data obtained from multiple individuals to demonstrate its practical applicability and robustness in real-world individual authentication scenarios (Figure 5).

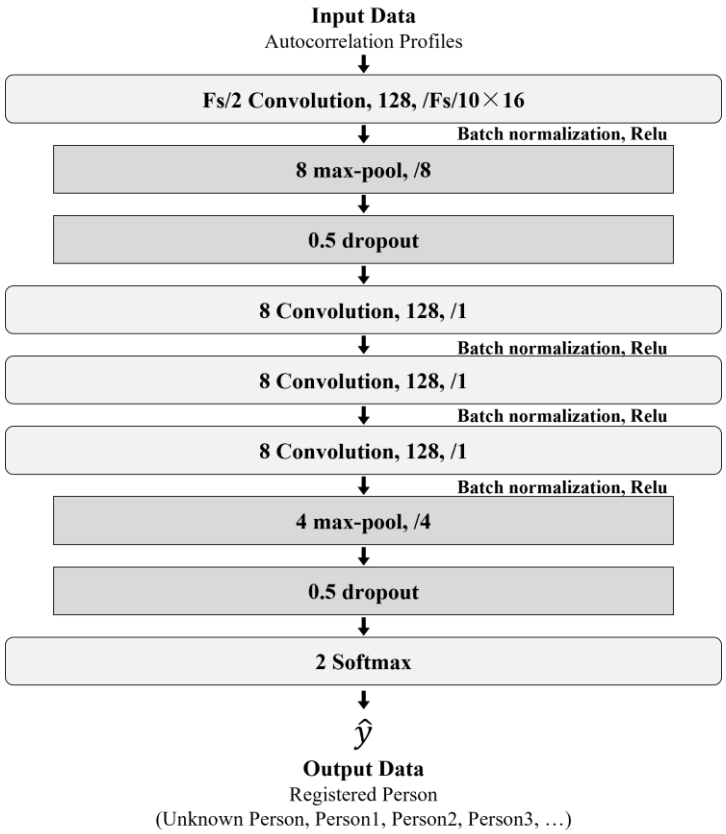


Figure 5. ECG learning network architecture for individual authentication.

3.4.1. Training Data Description

Open Data Validation:

The first dataset used to validate our learning architecture was sourced from the publicly available Haaglanden Medisch Centrum Sleep Staging Database v1.0.1, hosted by Physionet [47]. This dataset features ECG signals that were sampled at a frequency of 256 Hz using SOMNOscreen PSG, PSG+, and EEG 10-20 recording systems (SOMNOmedics, Randersacker, Germany) equipped with AgAgCl electrodes. The raw polysomnography (PSG) signals were digitalized in the EDF format, adhering to the basic analog pre-filter settings as per the device specifications. The scoring of sleep stages was manually executed by experienced sleep technicians based on the 2.4 version of the AASM guidelines [48]. This dataset helped confirm the efficacy of our model under varied conditions and with diverse ECG signal profiles.

Laboratory-Collected ECG Data for System Verification

The second dataset consists of ECG features derived from 10 individuals, collected in a controlled laboratory setting as described in Section 3.1 (ECG Measurement). This dataset was meticulously gathered to ensure high fidelity in signal acquisition, thus providing clear and consistent ACPs. These profiles are essential for training our model to recognize and

differentiate the unique ECG signatures of enrolled individuals, serving as the primary source for validating the model's capabilities in the enrollment and verification phases.

Together, these datasets not only enhance the diversity of our training data but also ensure that the model is robust and adaptable to different operational conditions and populations. This dual-dataset strategy effectively tests and hones the model's ability to function accurately in real-world authentication scenarios.

3.4.2. Network Architecture

The proposed CNN comprises several layers, each meticulously configured to optimize feature extraction and classification efficacy:

- Normalization and Activation Functions: Initial layers include batch normalization, which stabilizes learning by normalizing the input layers' activations. This ensures the mean activation is close to zero and the standard deviation near one, significantly enhancing the training process's stability. Non-linear activation functions, specifically rectified linear units (ReLUs) [49], follow these normalization layers to introduce necessary non-linear properties into the network, allowing for the learning of complex patterns within the data.
- Convolutional Layers: The core of the network consists of three convolutional layers, each equipped with 128 filters of size 8 and a stride of 1. These layers are pivotal in detecting intricate patterns and features in the ECG signal, providing a rich feature set for subsequent identification tasks.
- Pooling Layers: Spatial pooling (max-pooling) is employed twice within the network; initially with a kernel of 8 and stride of 8, followed by a second pooling stage with a kernel of 4 and stride of 4. These pooling operations reduce feature dimensionality, mitigate the risk of overfitting, and decrease computational demands by summarizing the features retained from prior convolutional layers.
- Dropout Regularization: To further guard against overfitting, dropout layers with a dropout rate of 0.5 are interspersed post-pooling. This probabilistic layer deactivates a random selection of neurons during training, which helps to eliminate minor dependencies in training data that might not generalize well to unseen data.
- Output Classification: The architecture culminates in a SoftMax classification layer. This layer categorizes the input ECG profiles into distinct classes, representing 'Registered Person' and 'Unknown Person', among others, by outputting probabilities that indicate the most likely class membership.

3.4.3. Training Parameters

The network was trained under the following specifications to ensure robust convergence and optimal performance:

- Epochs: Set to 300 to allow sufficient iterations over the training data for the network weights to converge towards effective discriminators;
- Learning Rate: A learning rate of 0.0001 was chosen, facilitated by the Adam optimization algorithm, renowned for its efficiency in handling sparse gradients and adaptive learning rate capabilities;
- Optimizer Configuration: Adam was configured with first and second moment estimates (beta1 of 0.9 and beta2 of 0.999, respectively), alongside a stability constant (epsilon of 1×10^{-8}) to prevent division by zero during updates [50];
- Gradient Clipping: Gradient values were clipped at 5 to prevent exploding gradients, a common issue in deep networks with deep architectures or large datasets;
- Regularization Strategy: An L2 regularization approach with a weight decay factor of 0.001 was implemented to penalize large weights, promoting simpler models less prone to overfitting.

This deep learning framework was devised to harness the unique characteristics of ECG signals, leveraging advanced machine learning techniques for effective and secure individual authentication. Incorporating these diverse datasets into our training regimen

enables the deep learning model to learn comprehensive feature representations, essential for achieving high accuracy in individual authentication based on ECG signals. The detailed architecture and learning parameters, as described in Sections 3.4.2 and 3.4.3, respectively, leverage the intricacies and the quality of the data provided in these datasets, ensuring optimal learning outcomes.

4. Results

4.1. Validation with Public Dataset

To validate the proposed individual authentication algorithm, two experiments were conducted. The first experiment utilized the publicly available HMC dataset [51,52] from the PhysioNet website, which comprises polysomnographic data from 154 individuals. This dataset includes various physiological signals such as electroencephalography, electrocardiography, electromyography, and electrooculography. In this study, we focused on electrocardiography data to evaluate the authentication efficiency of 154 individuals.

The data were acquired using wet electrodes with a sampling rate of 256 Hz through Somno-medics devices [51] and was downsampled to 100 Hz for the experiment. Approximately 8 h of sleep data were recorded daily, of which 6 h were used for training (enrollment) and the remaining 2 h for testing (verification). To further ensure robust validation, the 2 h test data were divided into 100 segments, and each segment was tested individually (Figure 6). Accuracy and F1-Scores were computed for each segment, allowing for a detailed evaluation of the algorithm's performance under varied conditions.

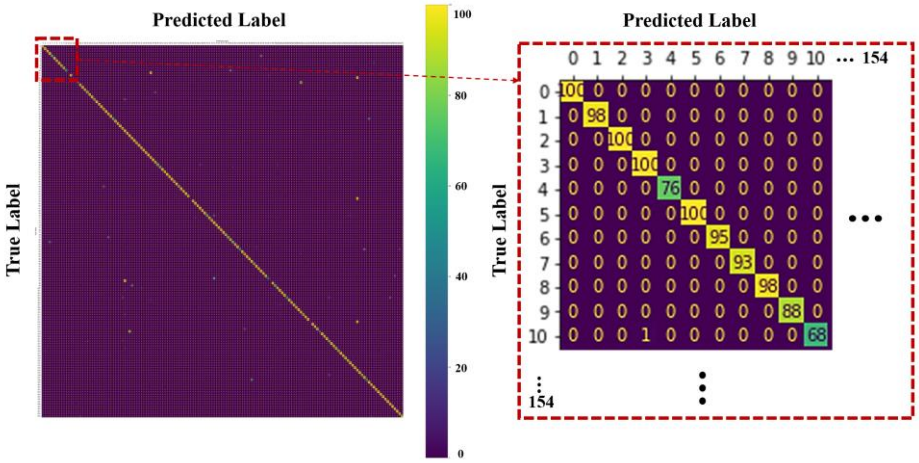


Figure 6. An example of a confusion matrix for calculating individual authentication efficiency is shown, where higher scores are represented in yellow and lower scores in green. Through a detailed evaluation of the 2 h test data divided into 100 segments, the proposed algorithm achieved an F1-Score of 96.8%.

The efficiency was assessed using a Confusion Matrix, achieving an F1-Score of 96.8%, as presented in Table 1. This score surpasses those reported in the comparative study [10], validating the effectiveness of the algorithm with a larger experimental group.

4.2. Validation with Steering Wheel Dataset

This study first validated the model's performance using the HMC dataset and subsequently ensured its reliability by utilizing an additional dataset collected from 10 participants. This approach enhanced the generalizability of the dataset through diverse applications and demonstrated that the model maintained high performance even in real-world scenarios [53]. This experiment involved acquiring ECG signals for individual authentication using dry electrodes attached to a vehicle's steering wheel. Figure 7a illustrates the configuration of the steering wheel, and Figure 7b shows an example of data acquisition. A total of 10 participants were involved, with ECG data collected for

30 min daily over 20 days. Out of these data, 8 h were used for training and 2 h for testing. Employing the 10-fold cross validation method, the average F1-Score obtained was 96.02%, as indicated in Table 2. Each validation process involved data segments of 5 s.

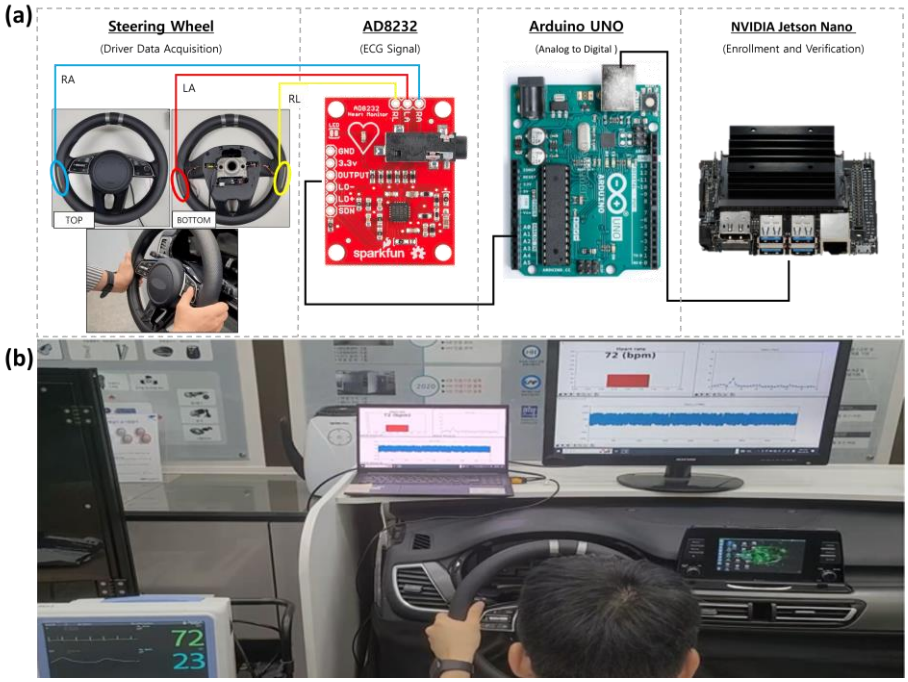


Figure 7. Individual authentication using a steering wheel: (**a**) steering wheel configuration and (**b**) example of steering wheel data acquisition.

Table 1. Comparison of individual authentication efficiencies.

Metric	HMC Open DB (Proposed)	Steering Wheel DB (Proposed)	Ref. [10]	Ref. [54]
F1-Score	96.80%	96.02%	96.40%	93.8% (Accuracy Rate)
Subject	154	10	100	10
Verification time (s)	5 s	5 s	10 s	10 s
Enroll Time (Total)	6 h	8 h	10~50 s	60 s
Test Time (Total)	2 h	2 h	10~30 s	60 s
Electrode	Wet electrode (SOMNO screen PSG equipment)	Dry electrode (ad8232)	Wet electrode (-)	Wet electrode (-)

Table 2. Individual authentication using a steering wheel (10-fold cross validation).

Subject	F1-Score	Subject	F1-Score
1	97.10%	6	95.70%
2	95.54%	7	95.93%
3	95.64%	8	96.94%
4	95.40%	9	96.51%
5	96.67%	10	95.78%
Average		96.02%	

5. Ablation Study

5.1. Effect of Component Removal on F1-Score

To evaluate the performance of the individual authentication system, an analysis was conducted by removing individual components and examining the resulting F1-Scores. The removal of ACPs led to a reduction in the F1-Score to 68.2%, demonstrating its critical role in capturing unique patterns from ECG signals. When the normalization step was removed, the F1-Score decreased to 85.4%, highlighting the importance of scaling data to a consistent range for reliable authentication results. Similarly, removing the BPF resulted in a drop in the F1-Score to 89.5%, underscoring the necessity of filtering to minimize noise and enhance signal clarity. Removing all components led to the lowest F1-Score of 60.1%, validating the cumulative importance of each component in the system. These results emphasize that each component plays a vital role in maintaining the system's overall accuracy. The ACPs and normalization are particularly crucial for achieving high accuracy, while the bandpass filter is essential for minimizing noise and enhancing signal clarity. This analysis underscores the necessity of each component within the ECG-based driver authentication system, highlighting that the integration of all components is essential for optimizing the system's performance and reliability in real-world scenarios.

5.2. Effect of Enrollment Time on F1-Score

Figure 8 presents the F1-Score of the individual authentication system based on different enrollment times using both the HMC dataset and an internally collected steering wheel dataset. The results in Figure 8 show a clear trend: longer enrollment times generally lead to higher authentication F1-Scores. For the HMC dataset, the F1-Score improves from 75.0% with a 1 min enrollment to 97.0% with an 8 h enrollment. Similarly, for the steering wheel dataset, the F1-Score increases from 61.0% to 96.0% over the same period.

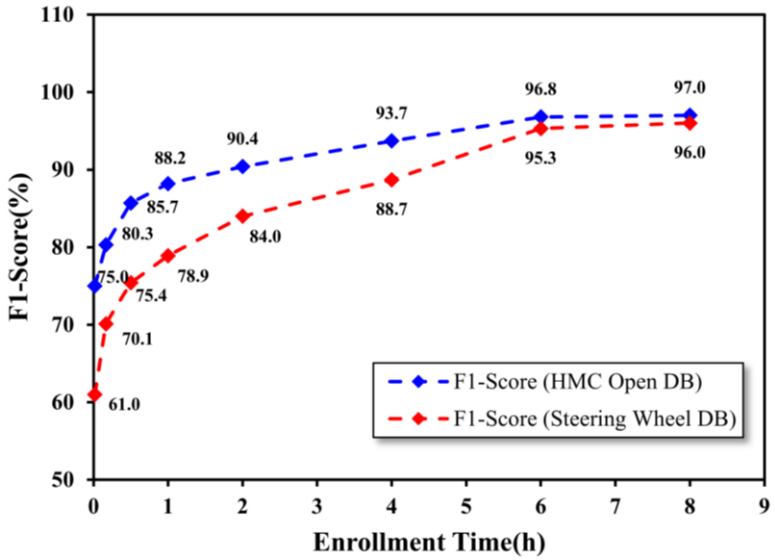


Figure 8. Effect of enrollment time on F1-Score for HMC open DB and steering wheel DB.

Notably, as the enrollment time increases, the system's efficiency gradually improves, but the improvement starts to plateau once the enrollment time exceeds 6 h. This suggests that, beyond 6 h, the additional enrollment time has diminishing returns on the system performance, indicating a convergence trend. Therefore, at least 6 h of data are required to ensure high performance, as further improvements in the F1-Score become marginal.

Longer enrollment periods allow the system to better adapt to individual variations and environmental factors, thereby enhancing the robustness of the individual authentication system. These findings highlight that, while longer enrollment times improve efficiency, the performance gains converge after 6 h, emphasizing the importance of setting

an optimal enrollment period. Future research should focus on identifying the minimum effective enrollment time that balances system performance and user convenience.

5.3. Effect of Model Size on F1-Score

To investigate the effect of model size on individual authentication systems, we evaluated various models in terms of accuracy and inference time. Our proposed 2D CNN model was compared against EECGNet, BiometricNet, BiGRU-ECG, AlexNet-ECG, GoogLeNet-ECG, and ResNet-34-ECG, focusing on model size (MB) and F1-Score (%). All these models are designed for ECG-based individual authentication [29–32,55–57].

The dataset was obtained from the HMC dataset, which includes ECG data from 154 participants. Models were trained and tested using 10-fold cross-validation. The results, shown in Figure 9, indicate that, as the model size increases, the F1-Score also improves. The proposed model's F1-Scores at different sizes are as follows: 11.8 MB (96.8%), 14.5 MB (97.3%), 18.2 MB (97.7%), 22.8 MB (98.1%), and 35.6 MB (98.5%).

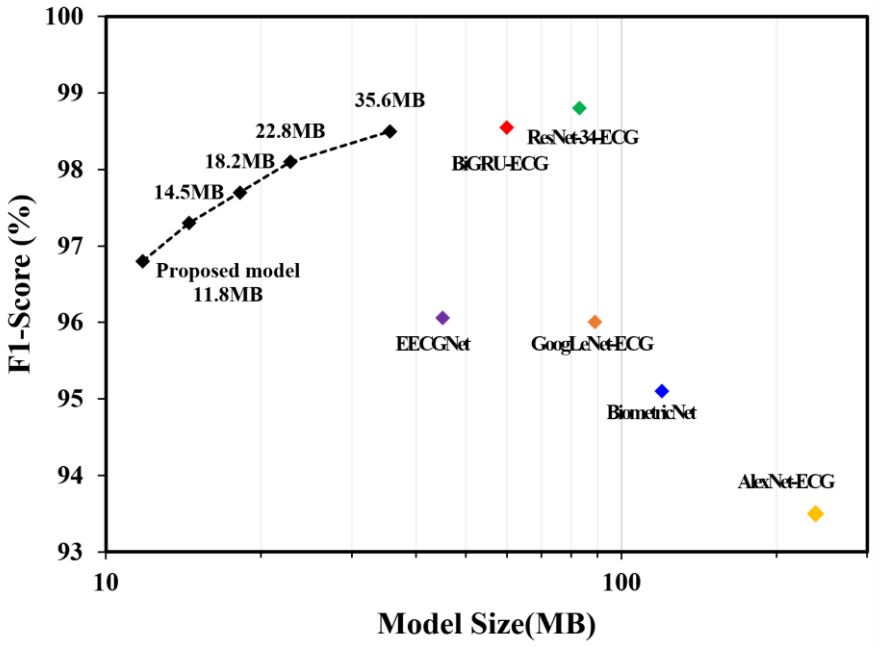


Figure 9. Impact of model size on F1-Score: comparison of different models using the HMC open database.

The computational cost of a convolution layer is proportional to the kernel size, the number of input channels, output channels, and the output length. Batch normalization and activation layers are also proportional to the output size and the number of output channels. In the case of max-pooling, the computational cost is proportional to the input length divided by the stride and the number of output channels. For dense layers, the computational cost is proportional to the input size and output size. Based on these calculations, the proposed learning model in this study has an estimated computational cost of approximately 3.85M FLOPs, with a corresponding model size of around 11.8 MB.

As shown in Figure 9, when the number of convolution layers in the middle layer (Layer 2) increases from 3 to 6, the model size approximately doubles to 22.8 MB, and the accuracy improves from 96.8% to 98.1%, an increase of about 1.3%. When the number of convolution layers increases from 3 to 9, the model size triples to approximately 35.6 MB, with an accuracy improvement of about 1.7%. In this study, the system is designed using a low-cost AI edge board, Jetson Nano. To minimize latency and ensure the user does not perceive delays, the number of convolution layers in the middle layer was set to 3.

Our model demonstrated clear advantages over other models in both accuracy and size. EECGNet (45 MB) achieved 96.06%, BiometricNet (120 MB) reached 95.10%, BiGRU-

ECG (60 MB) showed 98.55%, AlexNet-ECG (238 MB) achieved 93.50%, GoogLeNet-ECG (89 MB) reached 96.00%, and ResNet-34-ECG (83 MB) achieved 98.80%.

Figure 9 shows that our proposed model is significantly lighter than other models while maintaining high accuracy. Despite its smaller size, our model performs exceptionally well in classifying 154 participants based on the HMC dataset. The proposed model's compactness and high performance make it highly suitable for real-time applications in automotive environments, where computational efficiency and quick response times are critical.

These findings highlight the importance of optimizing model size without compromising accuracy. The lightweight nature of our model, combined with its high F1-Score, underscores its potential for practical deployment in ECG-based driver authentication systems. This analysis supports the proposed model's effectiveness in real-world scenarios.

6. Conclusions

This paper proposes a steering wheel system that can be used for individual authentication and bio-signal measurement, designed for integration within vehicles. The system enables the individual authentication algorithm to extract individual features through a fiducial-independent ACP, which eliminates the need for waveform identification, considering real-world application. After feature extraction, a lightweight CNN with a size of 11.8 M was used for training. This methodology successfully reduced the verification time to 5 s without significantly reducing the accuracy.

To test this algorithm, two datasets were utilized. The first experiment employed the publicly available HMC dataset, demonstrating superior F1-Score results compared to other studies using the same 5 s verification timeframe. In the second experiment, ECG data acquired from dry electrodes attached to a custom-built steering wheel were used. Despite dry electrodes being more susceptible to noise than wet electrodes, the combination of ACPs and CNN effectively prevented a reduction in the accuracy.

However, the individual authentication system proposed in this paper still requires a 5 s verification time and utilizes expensive Edge-AI boards for processing, which are substantial barriers to practical implementation. Future research will focus on network lightening and further reducing the verification time, enhancing the system's applicability and efficiency.

Author Contributions: Conceptualization, G.K. and T.J.; Software, G.K., C.Y. and J.J.; Validation, C.C.; Investigation, C.Y., P.K. and S.P.; Writing—original draft, J.J.; Writing—review & editing, G.K., P.K., S.P. and T.J.; Supervision, J.K.; Project administration, C.C. All authors have read and agreed to the published version of the manuscript.

Funding: This work was supported by Korea Innovation Foundation (RS-2024-00466949), funded by the Korean Ministry of Science and ICT.

Data Availability Statement: Data is contained within the article.

Conflicts of Interest: The authors declare no conflicts of interest.

References

1. Chen, Y.; Yin, J. Design of electroencephalogram authentication access control to smart car. *Healthc. Technol. Lett.* **2020**, *7*, 109–113. [CrossRef] [PubMed]
2. Mahetalia, J.; Mehta, R.; Varudandi, S.; Samdani, K. A Comparative Study on Gesture Recognition Systems for Car Infotainment Systems. In Proceedings of the 2018 IEEE International Conference on System, Computation, Automation and Networking, ICSCA 2018, Pondicherry, India, 6–7 July 2018. [CrossRef]
3. Verma, B.; Choudhary, A. A Framework for Driver Emotion Recognition using Deep Learning and Grassmann Manifolds. In Proceedings of the IEEE Conference on Intelligent Transportation Systems (ITSC), Maui, HI, USA, 4–7 November 2018; pp. 1421–1426. [CrossRef]
4. Ouda, A. A framework for next generation user authentication. In Proceedings of the 2016 3rd MEC International Conference on Big Data and Smart City, ICBDSC 2016, Muscat, Oman, 15–16 March 2016; pp. 97–100. [CrossRef]

5. Reese, K.; Smith, T.; Dutson, J.; Armknecht, J.; Cameron, J.; Seamons, K. A Usability Study of Five Two-Factor Authentication Methods. In Proceedings of the Fifteenth Symposium on Usable Privacy and Security (SOUPS 2019), Santa Clara, CA, USA, 11–13 August 2019. Available online: https://www.usenix.org/conference/soups2019/presentation/alqhatani (accessed on 25 April 2024).
6. Regani, S.D.; Xu, Q.; Wang, B.; Wu, M.; Liu, K.J.R. Driver Authentication for Smart Car Using Wireless Sensing. *IEEE Internet Things J.* **2020**, *7*, 2235–2246. [CrossRef]
7. Burge, M.; Burger, W. Ear Biometrics. In *Biometrics: Personal Identification in Networked Society*; Springer: Berlin/Heidelberg, Germany, 1996; pp. 273–285. [CrossRef]
8. Sanchit; Ramalho, M.; Correia, P.L.; Soares, L.D. Biometric identification through palm and dorSal hand vein patterns. In Proceedings of the EUROCON 2011—International Conference on Computer as a Tool—Joint with Conftele, Lisbon, Portugal, 27–29 April 2011. [CrossRef]
9. Kim, M.-G.; Ko, H.; Pan, S.B. A study on user recognition using 2D ECG based on ensemble of deep convolutional neural networks. *J. Ambient. Intell. Humaniz. Comput.* **2020**, *11*, 1859–1867. [CrossRef]
10. Choi, G.-H.; Bak, E.-S.; Pan, S.-B. User Identification System Using 2D Resized Spectrogram Features of ECG. *IEEE Access* **2019**, *7*, 34862–34873. [CrossRef]
11. Kim, M.-G.; Pan, S.B. Deep Learning Based on 1-D Ensemble Networks Using ECG for Real-Time User Recognition. *IEEE Trans. Ind. Inform.* **2019**, *15*, 5656–5663. [CrossRef]
12. Chu, Y.; Shen, H.; Huang, K. ECG Authentication method based on parallel multi-scale one-dimensional residual network with center and margin loss. *IEEE Access* **2019**, *7*, 51598–51607. [CrossRef]
13. Nayak, S.K.; Bit, A.; Dey, A.; Mohapatra, B.; Pal, K. A review on the nonlinear dynamical system analysis of electrocardiogram signal. *J. Healthc. Eng.* **2018**, *2018*, 6920420. [CrossRef]
14. Cheng, Y.; Yan, L.; Shoukat, M.U.; She, J.; Liu, W.; Shi, C.; Wu, Y.; Yan, F. An improved SSVEP-based brain-computer interface with low-contrast visual stimulation and its application in UAV control. *J. Neurophysiol.* **2024**, *132*, 809–821. [CrossRef]
15. Wahabi, S.; Pouryayevali, S.; Hatzinakos, D. Posture-invariant ECG recognition with posture detection. In Proceedings of the 2015 IEEE International Conference on Acoustics, Speech and Signal Processing (ICASSP), South Brisbane, QLD, Australia, 19–24 April 2015; pp. 1812–1816. [CrossRef]
16. Israel, S.A.; Irvine, J.M.; Cheng, A.; Wiederhold, M.D.; Wiederhold, B.K. ECG to identify individuals. *Pattern Recognit.* **2005**, *38*, 133–142. [CrossRef]
17. Irvine, J.M.; Israel, S.A. A sequential procedure for individual identity verification using ECG. *EURASIP J. Adv. Signal Process.* **2009**, *2009*, 243215. [CrossRef]
18. Aggarwal, A.; Badra, M.; Massacci, F. *Biometric Identification System Based on Electrocardiogram Data*; IEEE: Piscataway, NJ, USA, 2008.
19. Singh, Y.N.; Gupta, P. ECG to individual identification. In Proceedings of the 2008 IEEE Second International Conference on Biometrics: Theory, Applications and Systems, Washington, DC, USA, 29 September–1 October 2008. [CrossRef]
20. Singh, Y.N.; Gupta, P. Correlation-based classification of heartbeats for individual identification. *Soft Comput.* **2011**, *15*, 449–460. [CrossRef]
21. Yao, J.; Wan, Y. A wavelet method for biometric identification using wearable ECG sensors. In Proceedings of the 5th Int Workshop on Wearable and Implantable Body Sensor Networks, BSN2008, in Conjunction with the 5th Int Summer School and Symp on Medical Devices and Biosensors, ISSS-MDBS 2008, Hong Kong, China, 1–3 June 2008; pp. 297–300. [CrossRef]
22. Chan, A.D.C.; Hamdy, M.M.; Badre, A.; Badee, V. Wavelet distance measure for person identification using electrocardiograms. *IEEE Trans. Instrum. Meas.* **2008**, *57*, 248–253. [CrossRef]
23. Li, M.; Narayanan, S. Robust ECG biometrics by fusing temporal and cepstral information. In Proceedings of the International Conference on Pattern Recognition, Istanbul, Turkey, 23–26 August 2010; pp. 1326–1329. [CrossRef]
24. Zhang, Q.; Zhou, D.; Zeng, X. HeartID: A Multiresolution Convolutional Neural Network for ECG-Based Biometric Human Identification in Smart Health Applications. *IEEE Access* **2017**, *5*, 11805–11816. [CrossRef]
25. Boostani, R.; Sabeti, M.; Omranian, S.; Kouchaki, S. ECG-Based Personal Identification Using Empirical Mode Decomposition and Hilbert Transform. *Iran. J. Sci. Technol. Trans. Electr. Eng.* **2019**, *43*, 67–75. [CrossRef]
26. Zhao, Z.; Yang, L.; Chen, D.; Luo, Y. A human ECG identification system based onensemble empirical mode decomposition. *Sensors* **2013**, *13*, 6832–6864. [CrossRef]
27. Xu, J.; Li, T.; Chen, Y.; Chen, W. Personal Identification by Convolutional Neural Network with ECG Signal. In Proceedings of the 9th International Conference on Information and Communication Technology Convergence: ICT Convergence Powered by Smart Intelligence (ICTC), Jeju, Republic of Korea, 17–19 October 2018; pp. 559–563. [CrossRef]
28. Deshmane, M.; Madhe, S. ECG Based Biometric Human Identification Using Convolutional Neural Network in Smart Health Applications. In Proceedings of the 2018 4th International Conference on Computing, Communication Control and Automation, ICCUBEA, Pune, India, 16–18 August 2018. [CrossRef]
29. Hammad, M.; Pławiak, P.; Wang, K.; Acharya, U.R. ResNet-Attention model for human authentication using ECG signals. *Expert Syst.* **2021**, *38*, e12547. [CrossRef]

30. Lee, J.-N.; Byeon, Y.-H.; Pan, S.-B.; Kwak, K.-C. An EigenECG Network Approach Based on PCANet for Personal Identification from ECG Signal. *Sensors* **2018**, *18*, 4024. [CrossRef]
31. Lynn, H.M.; Pan, S.B.; Kim, P. A Deep Bidirectional GRU Network Model for Biometric Electrocardiogram Classification Based on Recurrent Neural Networks. *IEEE Access* **2019**, *7*, 145395–145405. [CrossRef]
32. Sateesh Kumar, T.R.; Purushottama, T.L. ECG Authentication Reinforced by Pretrained Convolutional Neural Networks. In Proceedings of the 2023 International Conference on Network, Multimedia and Information Technology, NMITCON, Bengaluru, India, 1–2 September 2023. [CrossRef]
33. Gomes, J.; Winters, S.L.; Stewart, D.; Targonski, A.; Barreca, P. Optimal bandpass filters for time-domain analysis of the signal-averaged electrocardiogram. *Am. J. Cardiol.* **1987**, *60*, 1290–1298. [CrossRef]
34. Luo, S.; Johnston, P. A review of electrocardiogram filtering. *J. Electrocardiol.* **2010**, *43*, 486–496. [CrossRef]
35. Nishimura, S.; Hirano, K.; Mitra, S.K. Design of Digital Notch Filters. *IEEE Trans. Commun.* **1974**, *22*, 964–970. [CrossRef]
36. Sathyapriya, L.; Murail, L.; Manigandan, T. Analysis and detection R-peak detection using Modified Pan-Tompkins algorithm. In Proceedings of the 2014 IEEE International Conference on Advanced Communication, Control and Computing Technologies, ICACCCT, Ramanathapuram, India, 8–10 May 2014; pp. 483–487. [CrossRef]
37. Fariha, M.A.Z.; Ikeura, R.; Hayakawa, S.; Tsutsumi, S. Analysis of Pan-Tompkins Algorithm Performance with Noisy ECG Signals. *J. Phys. Conf. Ser.* **2020**, *1532*, 012022. [CrossRef]
38. Choi, H.-S.; Lee, B.; Yoon, S. Biometric Authentication Using Noisy Electrocardiograms Acquired by Mobile Sensors. *IEEE Access* **2016**, *4*, 1266–1273. [CrossRef]
39. Krasteva, V.; Jekova, I.; Abächerli, R. Biometric verification by cross-correlation analysis of 12-lead ECG patterns: Ranking of the most reliable peripheral and chest leads. *J. Electrocardiol.* **2017**, *50*, 847–854. [CrossRef]
40. da Silva, H.P.; Lourenço, A.; Fred, A.; Raposo, N.; Aires-De-Sousa, M. Check Your Biosignals Here: A new dataset for off-the-person ECG biometrics. *Comput. Methods Programs Biomed.* **2014**, *113*, 503–514. [CrossRef]
41. Dong, J.; Jiang, W. Design of digital filter on ECG signal processing. In Proceedings of the 5th International Conference on Instrumentation and Measurement, Computer, Communication, and Control, IMCCC, Qinhuangdao, China, 18–20 September 2015; pp. 1272–1275. [CrossRef]
42. Marzog, H.A.; Abd, H.J.; Yonis, A. Noise Removal of ECG signal using Multi-Techniques. In Proceedings of the 2022 IEEE Integrated STEM Education Conference, ISEC, Princeton, NJ, USA, 26 March 2022; pp. 397–403. [CrossRef]
43. Plataniotis, K.N.; Hatzinakos, D.; Lee, J.K.M. ECG biometric recognition without fiducial detection. In Proceedings of the 2006 Biometrics Symposium: Special Session on Research at the Biometric Consortium Conference, Baltimore, MD, USA, 19 September–21 August 2006. [CrossRef]
44. Matta, R.; Lau, J.K.H.; Agrafioti, F.; Hatzinakos, D. Real-time continuous identification system using ECG signals. In Proceedings of the Canadian Conference on Electrical and Computer Engineering, Niagara Falls, ON, Canada, 8–11 May 2011; pp. 001313–001316. [CrossRef]
45. Yang, C.; Ku, G.W.; Lee, J.-G.; Lee, S.-H. Interval-Based LDA Algorithm for Electrocardiograms for Individual Verification. *Appl. Sci.* **2020**, *10*, 6025. [CrossRef]
46. Supratak, A.; Guo, Y. TinySleepNet: An Efficient Deep Learning Model for Sleep Stage Scoring based on Raw Single-Channel EEG. In Proceedings of the 2020 42nd Annual International Conference of the IEEE Engineering in Medicine & Biology Society (EMBC), Montréal, QC, Canada, 20–24 July 2020; pp. 641–644. [CrossRef]
47. Goldberger, A.L.; Amaral, L.A.N.; Glass, L.; Hausdorff, J.M.; Ivanov, P.C.; Mark, R.G.; Mietus, J.E.; Moody, G.B.; Peng, C.-K.; Stanley, H.E. PhysioBank, PhysioToolkit, and PhysioNet: Components of a new research resource for complex physiologic signals. *Circulation* **2000**, *101*, E215. [CrossRef]
48. Berry, R.B.; Brooks, R.; Gamaldo, C.; Harding, S.M.; Lloyd, R.M.; Quan, S.F.; Troester, M.T.; Vaughn, B.V. AASM Scoring Manual Updates for 2017 (Version 2.4). *J. Clin. Sleep Med.* **2017**, *13*, 665–666. [CrossRef]
49. Nair, V.; Hinton, G.E. Rectified Linear Units Improve Restricted Boltzmann Machines. In Proceedings of the 27th international conference on machine learning (ICML-10), Haifa, Israel, 21–24 June 2010.
50. Kingma, D.P.; Ba, J.L. Adam: A Method for Stochastic Optimization. In Proceedings of the 3rd International Conference on Learning Representations, ICLR 2015Conference Track Proceedings, San Diego, CA, USA, 7–9 May 2015; Available online: https://arxiv.org/abs/1412.6980v9 (accessed on 30 April 2024).
51. Haaglanden Medisch Centrum Sleep Staging Database v1.1. 2024. Available online: https://physionet.org/content/hmc-sleep-staging/1.1/ (accessed on 30 April 2024).
52. Mi, P.; Yan, L.; Cheng, Y.; Liu, Y.; Wang, J.; Shoukat, M.U.; Yan, F.; Qin, G.; Han, P.; Zhai, Y. Driver Cognitive Architecture Based on EEG Signals: A Review. *IEEE Sens. J.* **2024**, *24*, 36261–36286. [CrossRef]
53. Laganà, F.; Pratticò, D.; Angiulli, G.; Oliva, G.; Pullano, S.A.; Versaci, M.; La Foresta, F. Development of an Integrated System of sEMG Signal Acquisition, Processing, and Analysis with AI Techniques. *Signals* **2024**, *5*, 476–493. [CrossRef]
54. One-Lead Electrocardiogram for Biometric Authentication Using Time Series Analysis and Support Vector Machine. Available online: https://thesai.org/Publications/ViewPaper?Volume=10&Issue=2&Code=ijacsa&SerialNo=37 (accessed on 3 December 2024).
55. Yaacoubi, C.; Besrour, R.; Lachiri, Z. A multimodal biometric identification system based on ECG and PPG signals. In Proceedings of the 2nd International Conference on Digital Tools & Uses Congress, Manouba, Tunisia, 15–17 October 2020. [CrossRef]

56. Zheng, M.; Crouch, M.S.; Eggleston, M.S. Surface Electromyography as a Natural Human-Machine Interface: A Review. *IEEE Sens. J.* **2022**, *22*, 9198–9214. [CrossRef]
57. Ali, A.; Testa, M.; Bianchi, T.; Magli, E. BioMetricNet: Deep Unconstrained Face Verification Through Learning of Metrics Regularized onto Gaussian Distributions. In *Lecture Notes in Computer Science (Including Subseries Lecture Notes in Artificial Intelligence and Lecture Notes in Bioinformatics)*; Springer: Berlin/Heidelberg, Germany, 2020; pp. 133–149. [CrossRef]

Disclaimer/Publisher's Note: The statements, opinions and data contained in all publications are solely those of the individual author(s) and contributor(s) and not of MDPI and/or the editor(s). MDPI and/or the editor(s) disclaim responsibility for any injury to people or property resulting from any ideas, methods, instructions or products referred to in the content.